

The energy dependence of directed and elliptic flow

Hannah Petersen, Qingfeng Li, and Marcus Bleicher

Institut für Theoretische Physik and FIAS, Universität Frankfurt, Max-von-Laue-Straße 1, D-60438 Frankfurt am Main, Germany

Abstract

The energy excitation functions of v_1 and v_2 from $E_{\text{beam}} = 90A$ MeV to $E_{\text{cm}} = 200A$ GeV are explored within the UrQMD transport approach and discussed in the context of the available data. It is found that, in the energy regime below $E_{\text{beam}} \leq 10A$ GeV, the inclusion of nuclear potentials is necessary to describe the data. Above $40A$ GeV beam energy, the UrQMD model starts to underestimate the elliptic flow. Around the same energy the slope of the rapidity spectra of the proton directed flow develops negative values. This effect is known as the third flow component ("antiflow") and cannot be reproduced by the transport model. These differences can possibly be explained by assuming a phase transition from hadron gas to quark gluon plasma at about $40A$ GeV. This poster is based on the following publications [1, 2, 3].

The UrQMD model

For our investigation, the Ultra-relativistic Quantum Molecular Dynamics model (UrQMD v2.2) [4, 5] is applied to heavy ion reactions from $E_{\text{beam}} = 90A$ MeV to $\sqrt{s_{NN}} = 200$ GeV. This microscopic transport approach is based on the covariant propagation of constituent quarks and diquarks accompanied by mesonic and baryonic degrees of freedom. It simulates multiple interactions of in-going and newly produced particles, the excitation and fragmentation of colour strings and the formation and decay of hadronic resonances. A phase transition to a quark-gluon state is not incorporated explicitly into the model dynamics. The UrQMD transport model is successful in describing the yields and the p_t spectra of different particles in pp and pA collisions [6].

Time evolution

Let us now explore the time evolution of the pressure gradients in connection with the elliptic flow development. The transverse pressure gradients have been calculated for the first 10 fm at $E_{\text{lab}} = 40A$ GeV (see Figure 1(top)).

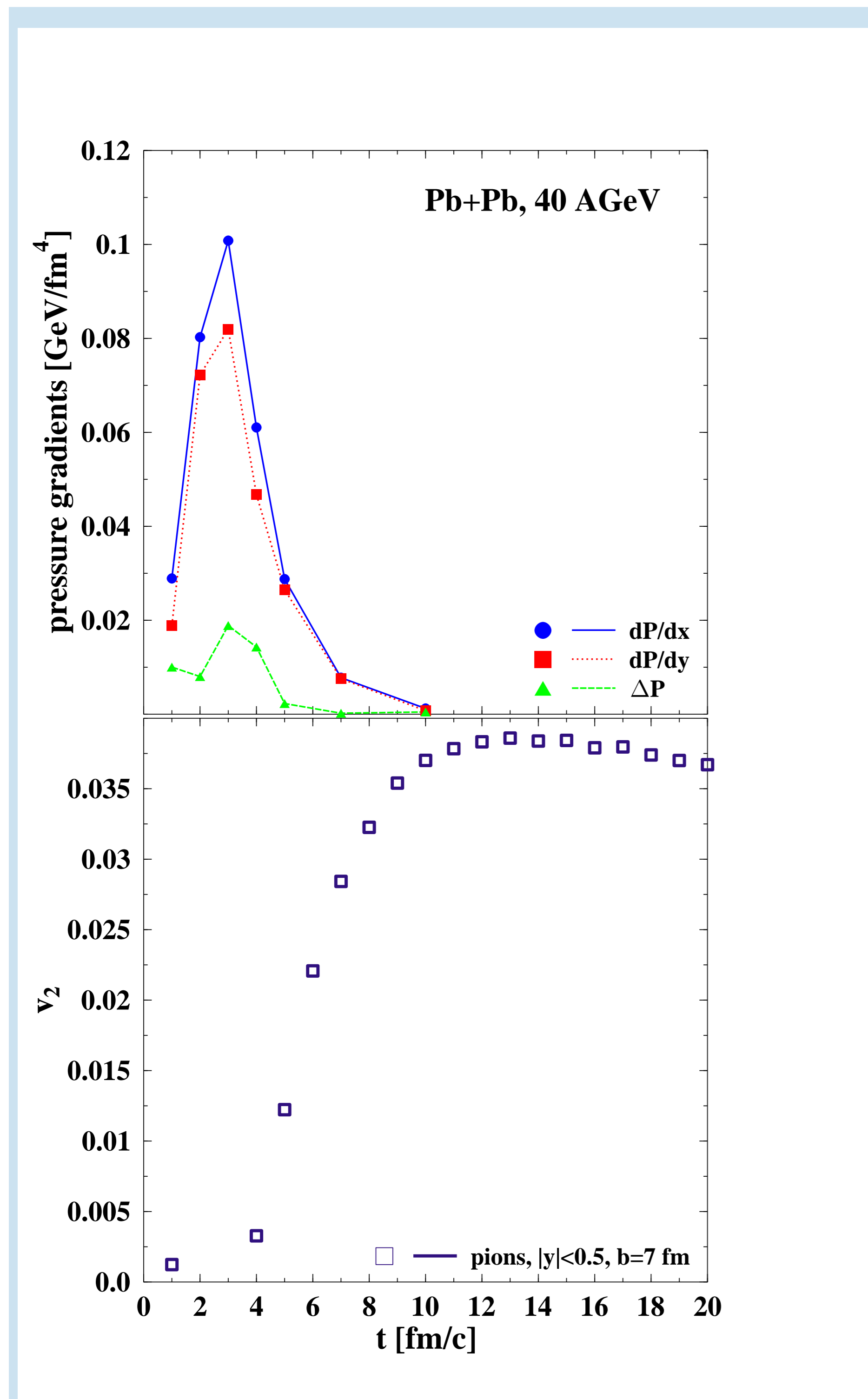


Figure 1: UrQMD calculation for the time evolution of the pressure gradients and elliptic flow for Pb+Pb interactions at $E_{\text{lab}} = 40A$ GeV. Top: dP/dx (full line), dP/dy (dotted line) and the difference between these two ΔP (dashed line) are depicted. Bottom: Elliptic flow of pions (squares) versus time at midrapidity for mid-central collisions ($b=7$ fm).

One observes large pressure gradients in the very early stage of the collision. The maximum is reached around $t = 3$ fm. The difference between the pressure gradients in x- and y- direction is responsible for the v_2 development. As it can be seen in Figure 1(bottom) the temporal evolution of elliptic flow for pions starts exactly after this maximum. The elliptic flow increases during ~ 6 fm until it reaches almost its final value. After $t = 10$ fm it decreases a little because of resonance decays. So, elliptic flow builds up in the early stage of the collision due to the difference of pressure gradients as it is expected.

Directed flow

To characterize the amount and the direction of the directed flow of protons over the energy range from 2 – $160A$ GeV one can extract the slope around midrapidity from the normalized rapidity distributions usually referred to as the "F" parameter [7].

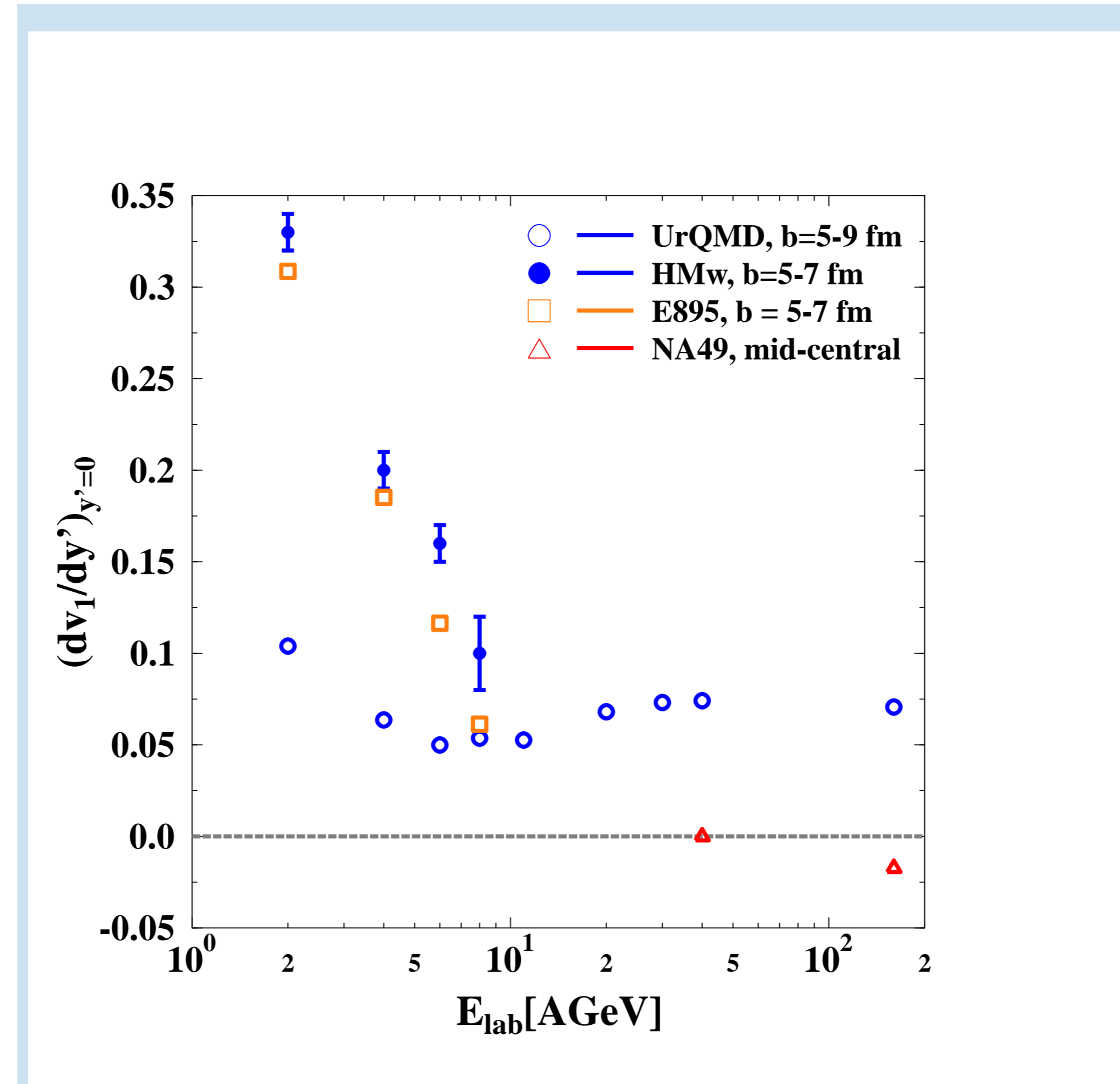


Figure 2: Slope of $v_1(y)$ of protons around midrapidity extracted from normalized ($y' = y/y_0$) rapidity distributions. The data are taken from E895 (squares) [7] and NA49 (triangles) [8]. UrQMD calculations with included mean field (HMw) are depicted with full circles. Open circles depict UrQMD calculation in the cascade mode.

In Figure 2 one observes that at lower energies the inclusion of a nuclear potential is needed to reproduce the data [9]. At SPS energies the data develop even negative values for the slope around midrapidity. This behaviour cannot be reproduced within the transport model calculation (cascade mode). However, ideal hydro calculations have predicted the appearance of a so-called "third flow component" [10] or "antiflow" at finite impact parameters. In these analysis' it was pointed out that this "antiflow" develops if the matter undergoes a first order phase transition to the QGP. In contrast, a hadronic EoS without QGP phase transition did not yield such an exotic "antiflow" (negative slope) wiggle in the proton flow $v_1(y)$ at low energies.

Elliptic flow

The excitation function of charged particle elliptic flow is compared to data over a wide energy range (Figure 3), i.e. from $E_{\text{lab}} = 90A$ MeV to $\sqrt{s_{NN}} = 200$ GeV.

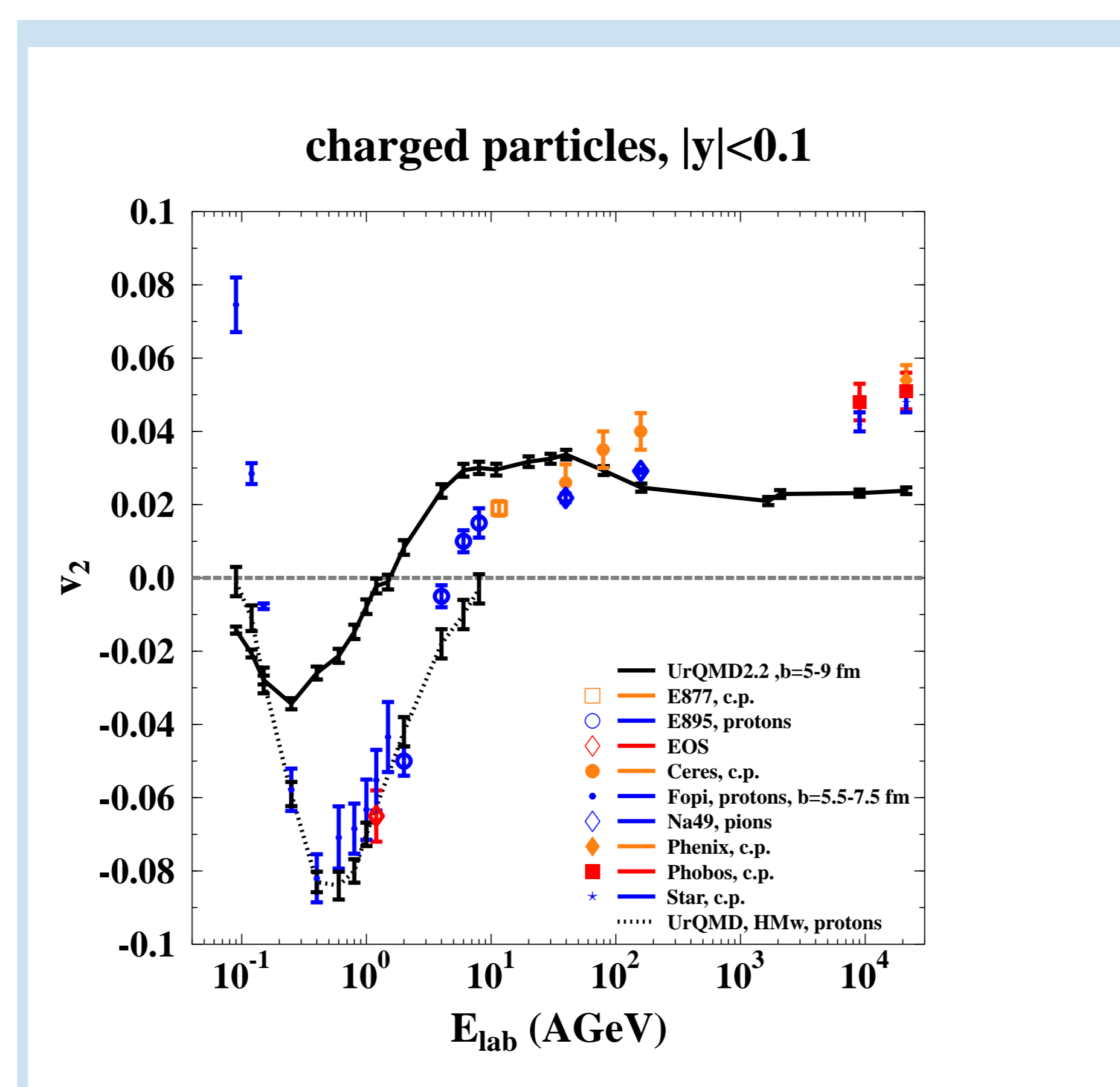


Figure 3: The calculated energy excitation function of elliptic flow of charged particles in Au+Au/Pb+Pb collisions in mid-central collisions ($b=5-9$ fm) with $|y| < 0.1$ (full line). This curve is compared to data from different experiments for mid-central collisions. For E895 [11, 12] and FOPI [13] there is the elliptic flow of protons and for NA49 [8] it is the elliptic flow of pions. For E877, CERES [14, 15, 16], PHENIX [17], PHOBOS [18] and STAR [19] there is data for the charged particle flow. The dotted line in the low energy regime depicts UrQMD calculations with the mean field [9].

The squeeze-out effect at low energies and the change to in-plane emission at higher energies is nicely observed in the excitation function. The symbols indicate the data for charged particles from different experiments. At low energies $E_{\text{beam}} \sim 0.1 - 6A$ GeV we adopt a hard equation of state with momentum dependence (HM-EoS) which was updated recently in the UrQMD model [9].

In the SPS regime the model calculations are quite in line with the data, especially with the NA49 results. Above $E_{\text{lab}} = 160A$ GeV the calculation underestimates the elliptic flow. At the highest RHIC energy there are about 5% flow in the data while the model calculation provides only half of this value. This can be explained by assuming a lack of pressure in the transport model at these energies.

Partonic fraction

It is possible that above the energy range about $E_{\text{lab}} = 40$ AGeV partonic interactions have to be taken into account to describe the data. To illuminate this, we have calculated the energy density during heavy ion collisions at different beam energies. From this, we extract the time corresponding to the maximum value of the total energy density.

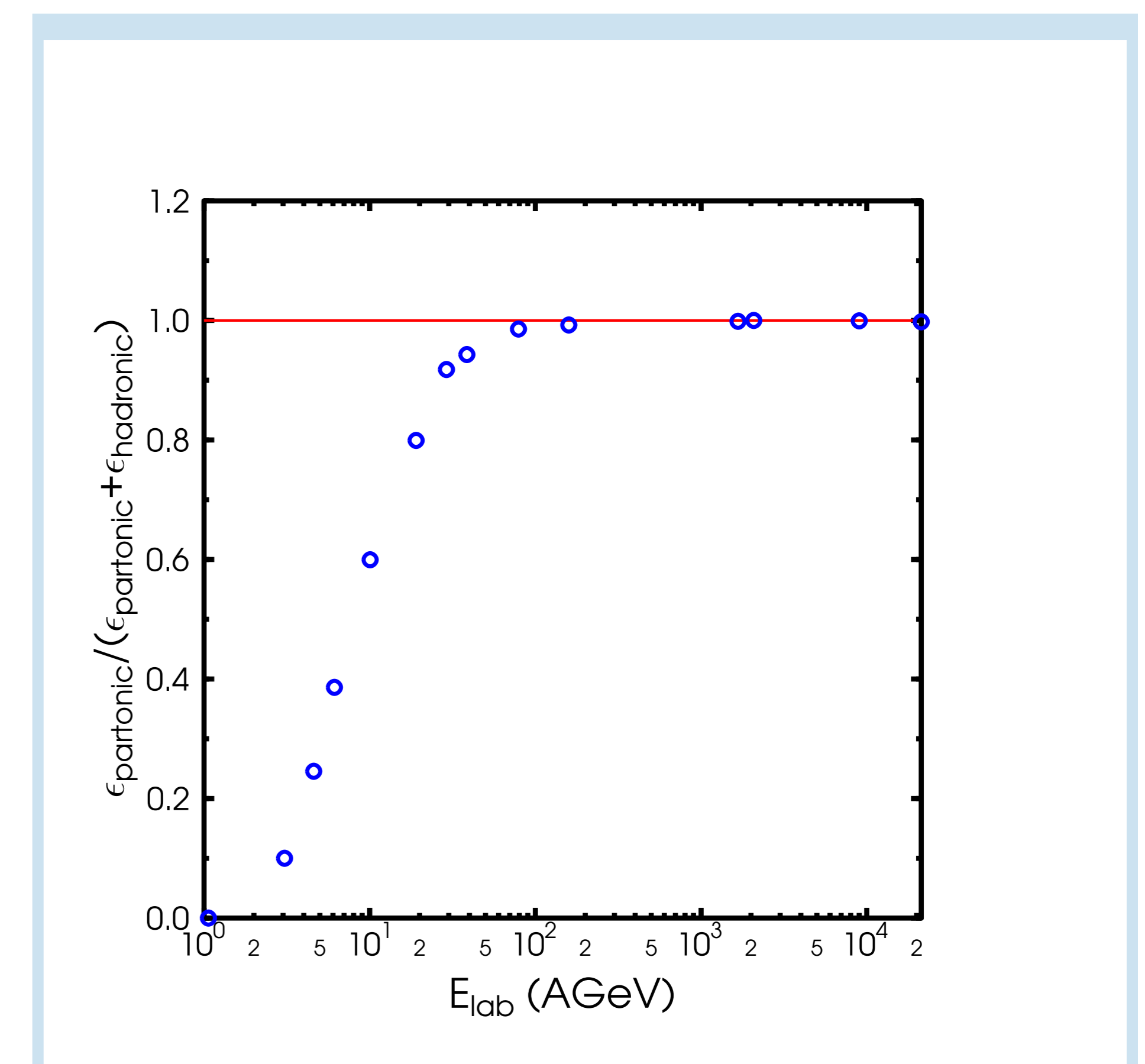


Figure 4: Calculated fraction of energy density in unformed hadrons with $|y| < 0.5$ and in a cylindrical volume with transverse radius $r = 3$ fm and length $h = 3/\gamma_{CM}$ fm as a function of the beam energy for central Pb+Pb (Au+Au) reactions.

Figure 4 shows the fraction of the energy density that is deposited in the "unformed hadrons" ($\epsilon_{\text{partonic}} / (\epsilon_{\text{partonic}} + \epsilon_{\text{hadronic}})$). I.e. all string fragments within their formation time are dubbed as 'partonic'. The fraction of $\epsilon_{\text{partonic}}$ starts at zero for low energies and then rises fast to almost 100%. Note that this fraction reaches 90% already around $40A$ GeV beam energy, similar to the energy region where a phase transition is expected. As one can see, the energy density of the formed hadrons ($\epsilon_{\text{hadronic}}$) is much smaller than the total value, therefore the effective pressure of the formed hadrons alone in the model seems to be too small to generate enough v_2 . Thus, this finding supports the interpretation of the need for initial pressure from "pre-QGP" matter already at low SPS energies.

Acknowledgements

We are grateful to the Center for the Scientific Computing (CSC) at Frankfurt for the computing resources. The authors thank Horst Stöcker for fruitful discussions. H. Petersen thanks the Deutsche Telekom Stiftung for the scholarship and the Helmholtz Research School on Quark Matter Studies for support. Q. Li thanks the Alexander von Humboldt-Stiftung for a fellowship. This work was supported by GSI and BMBF.

References

- [1] H. Petersen, Q. Li, X. Zhu and M. Bleicher, Phys. Rev. C 74 (2006) 064908
- [2] H. Petersen and M. Bleicher, Eur. Phys. J. C 49 (2007) 91.
- [3] X. Zhu, H. Petersen and M. Bleicher, AIP Conf. Proc. 828 (2006) 17.
- [4] M. Bleicher *et al.*, J. Phys. G 25 (1999) 1859
- [5] S. A. Bass *et al.*, Prog. Part. Nucl. Phys. 41 (1998) 225
- [6] E. L. Bratkovskaya *et al.*, Phys. Rev. C 69 (2004) 054907
- [7] H. Liu *et al.* [E895 Collaboration], Phys. Rev. Lett. 84 (2000) 5488
- [8] C. Alt *et al.* [NA49 Collaboration], Phys. Rev. C 68 (2003) 034903
- [9] Q. Li, Z. Li, S. Soff, M. Bleicher and H. Stöcker, J. Phys. G: Nucl. Part. Phys. 32, 151 (2006)
- [10] L. P. Csernai and D. Rohrlich, Phys. Lett. B 458 (1999) 454
- [11] C. Pinkenburg *et al.* [E895 Collaboration], APS meeting 1999
- [12] P. Chung *et al.* [E895 Collaboration], Phys. Rev. C 66 (2002) 021901
- [13] A. Andronic *et al.* [FOPI Collaboration], Phys. Lett. B 612 (2005) 173
- [14] K. Filimonov *et al.* [CERES/NA45 Collaboration], arXiv:nucl-ex/0109017.
- [15] J. Slivova [CERES/NA45 Collaboration], Nucl. Phys. A 715 (2003) 615
- [16] S.I. Esumi, J. Slivova, J. Milosevic for CERES Collaboration SFIN, year XV, Series A: Conferences, No. A2(2002)
- [17] S. Esumi [PHENIX Collaboration], Nucl. Phys. A 715 (2003) 599
- [18] S. Manly *et al.* [PHOBOS Collaboration], Nucl. Phys. A 715 (2003) 611
- [19] R. L. Ray [STAR Collaboration], Nucl. Phys. A 715 (2003) 45